ELSEVIER

Diamond and Related Materials 11 (2002) 8–15

DIAMOND AND RELATED MATERIALS

www.elsevier.com/locate/diamond

Structure of nitrogenated amorphous carbon films from NEXAFS

Somnath Bhattacharyya*, M. Lübbe, P.R. Bressler, D.R.T. Zahn, F. Richter

Institut für Physik, TU Chemnitz, D-09107 Chemnitz, Germany

Received 16 March 2001; accepted 9 May 2001

Abstract

The change in the structure of tetrahedral amorphous carbon (ta-C) films by nitrogen incorporation is studied by near-edge X-ray absorption fine structure (NEXAFS) spectroscopy and electron energy-loss spectroscopy (EELS). NEXAFS spectroscopy can be used to determine the molecular structure of amorphous nitrogenated carbon (a-CN_x) films due to its superior energy resolution as compared to EELS. This shows the structure of the films to be close to pyridine. The N K-edge spectra obtained from these spectroscopic techniques are decomposed into several peaks in order to compare the film structure after nitrogen incorporation. A comparative and combined study of NEXAFS spectroscopy and EELS reveals that as the nitrogen concentration in the films increases, the peaks π^* and σ^* at the C K-edge move towards higher energy and the π^*/σ^* intensity ratio at both edges decreases. These results indicate that there is an increase in the concentration of C=C and C=N relative to C–C and C–N bonds with nitrogen concentration, respectively. The difficulty of nitrogen doping of ta-C is also interpreted from the ratio of π^* and σ^* at C and N K-edges.

PACS: 61.10 Ht; 61.14.-x; 61.43.-j; 81.05. Tp

Keywords: Tetrahedral amorphous carbon; Carbon nitride; Near-edge X-ray absorption fine structure (NEXAFS); Density of states

1. Introduction

Near-edge X-ray absorption fine structure (NEXAFS) spectroscopy has been widely used for the investigation of the local atomic structure of many covalently bonded semiconductors, such as silicon and germanium [1–3]. This technique is also very sensitive to the chemisorbed molecular structure (such as benzene and pyridine) and has provided valuable information on the bond orientation of organic molecules [4–6]. Recently, the range of applications of NEXAFS spectroscopy has been greatly extended in the study of adsorption of medium and large symmetrical organic molecules [7]. In the field of carbon, NEXAFS spectroscopy has been successfully utilized for the structure determination of diamond and graphite [1], but for amorphous carbon (a-C), amorphous hydrogenated carbon (a-C:H), and particularly amorphous nitrogenated carbon (a-CN_x) films, this technique has not been extensively used. Due to the complex structure of CN_x films, several researchers have very recently shown interest in using NEXAFS spectroscopy to understand the local adsorption geometry of CN on metal surfaces [8]. In addition, NEXAFS has been used for the determination of the percentage of hybridization bonds in CN_x films, because the lack of long-range order and disorder in these films does not hinder the technique [9,10]. Considering the structure of CN_x films, and to some extent analogous to certain organic molecules, NEXAFS could be very useful in determining the structure of the N K-edge. Several researchers have been trying to understand the CN bonding arrangement from a comparative study between the shape and relative intensity of the C and N K-edges [11–14]. A dissimilarity between the shape of these edges may explain the fact that the type of bonding and environment of the C and N atoms are different [15–22].

On the other hand, techniques such as electron energy-loss spectroscopy (EELS) or electron energy-loss reflection fine-structure (EELFS) have also been used as complementary and powerful techniques for recording inner shell spectra at surfaces and in thin films [23]. The change in the local structure of ta-C films after incorporation of nitrogen has been previously described

* Corresponding author. Present address: 104 Davey Lab, The Pennsylvania State University, University Park, PA 16802, USA.
E-mail address: sub3@psu.edu (S. Bhattacharyya).

0925-9635/02/$ - see front matter
PII: S0925-9635(01)00525-8

using EELS spectra, where the fine structure of the K-edges was not resolved [11–14]. Recently, in combination with transmission electron microscopy (TEM), EELS was found to be very successful in determining local structures (in the nanometer range) of nitrogenated carbon films [15–20]. A combined study using NEXAFS and TEM has also been performed which could separate out different bond phases, even at the nanometer level [9,24]. With the help of NEXAFS spectroscopy together with high-resolution scanning electron microscopy (HRSEM), the formation of nanocrystalline diamond and its transformation by annealing was successfully demonstrated [25]. As the spectral resolution of NEXAFS spectroscopy is higher than that of EELS at the K-edges, a very clear understanding of the local bonding arrangement in the vicinity of the N and C atoms can be obtained from the detailed structure and a comparison between the intensity ratio of π^* and σ^* at these edges.

In the present report, we are primarily interested in investigating the structure of CN_x films independently by NEXAFS spectroscopy and EELS measurements. Another objective was to improve our previous interpretation of the CN_x film structure carried out by EELS [15–20] by analyzing NEXAFS spectra on similar samples. In this regard, a comparative and combined study using both methods is presented.

2. Experimental

The details of sample preparation and EELS experiments are given elsewhere [15–20]. Briefly, a filtered cathodic arc from a graphite target was applied and nitrogen was introduced into the films by admittance of a gas flow or by the bombardment of the growing film with nitrogen ions from a Kaufman-ion source (see Table 1). For a discharge voltage of 50 V for the ion source, the ratio of the N/C atom arrival rates (Q_r) was found to follow the relationship $Q_r = 1.7 \times j_N / j_C$, where j_N and j_C represent the current density of the nitrogen and carbon ions, respectively. The gas pressure in the chamber was maintained at approximately 2×10^{-4} Pa. The films were deposited on silicon (100) substrates that had been cleaned by ethanol and an argon ion beam. The average thickness of the films was approximately 40 nm. The stoichiometry and density of all the films were determined by elastic recoil-detection analysis (ERDA).

The electron energy-loss spectra were recorded using a Gatan 666 parallel EELS spectrometer mounted on a Philips CM20 FEG transmission electron microscope with primary electron energy of 200 keV. The point and line resolution of the microscope is 2.4 and 1.4 Å, respectively, and energy resolution of the spectrometer is approximately 1 eV. The spectral data were analyzed by GATAN EL/P version 2.1 software to correct for multiple scattering by dividing the Fourier transform of the K-shell spectrum by the corresponding Fourier transform of the low-loss spectrum, followed by an inverse Fourier transformation (Fourier-ratio method) [15–20].

Table 1
Description of the sample preparation conditions and nitrogen atomic concentration

Sample	N at.%	Preparation conditions	Q_r
ta-C	0	C^+ arc only	–
a-CN_{04}	4	C^+ arc + N_2 flow (3 sccm)	–
a-CN_{09}	9	C^+ arc + N_2 flow (20 sccm)	–
a-CN_{12}	12	C^+ arc + N^+/N_2^+ ions + 3 sccm N_2	0.08
a-CN_{19}	19	C^+ arc + N^+/N_2^+ ions + 3 sccm N_2	0.17
a-CN_{23}	23	C^+ arc + N^+/N_2^+ ions + 3 sccm N_2	0.25

The subscript 'x' of a-CN_x denotes the atomic concentration. N^+/N_2^+ ions were from a Kaufman ion source.

NEXAFS measurements were performed using the synchrotron radiation facility BESSY I in Berlin. The resolution of the CL-RCM beam line was 0.1 and 0.2 eV at the C and N K-edges, respectively. A nitrogen gas cell at a pressure of 5×10^{-3} mbar was used to record the flux curve. The spectra at C and N K-edges were recorded in total electron-yield mode and were normalized by dividing the flux curve. The jump of the C and N K-edges at the ionization potential was fitted by an erf function multiplied by an exponential decay function [1–3]. Although the ionization potential may be different for samples containing very different values of nitrogen, for simplicity it is considered as constant. The spectra after subtracting the respective jumps at both edges are decomposed into several Gaussian peaks. For fitting of the σ^* peak, asymmetric Gaussian peaks were used, following the previous reports [1–3]. The positions of the decomposed peaks were chosen, bearing in mind the peaks appearing in diamond, graphite and different organic molecules containing nitrogen.

3. Results and discussion

3.1. K edges from NEXAFS spectra

The NEXAFS and EELS spectra of C and N K-edges are presented in Fig. 1a–c and Fig. 2a,b, respectively. In NEXAFS, the peak corresponding to the $1s \rightarrow \pi^*$ transition at the C K-edge of ta-C appears at 284.5 eV. We carefully investigated the fine structure of the K-edges, which appear as a mixture of different features (see Fig. 1a,b). As ta-C is a sp^3-bonded carbon-rich system, it is reasonable to compare its C K-edge with that of diamond, also plotted in Fig. 1a and obtained from a report by Comelli et al. [3]. The main features of NEXAFS of diamond are: (i) a weak peak at ~285 eV (due to small sp^2 defects); (ii) an absorption edge at ~290 eV; (iii) a peak at ~297 eV ($1s \rightarrow \sigma^*$ transition); and (iv) a dip at ~302.5 eV (second bandgap).

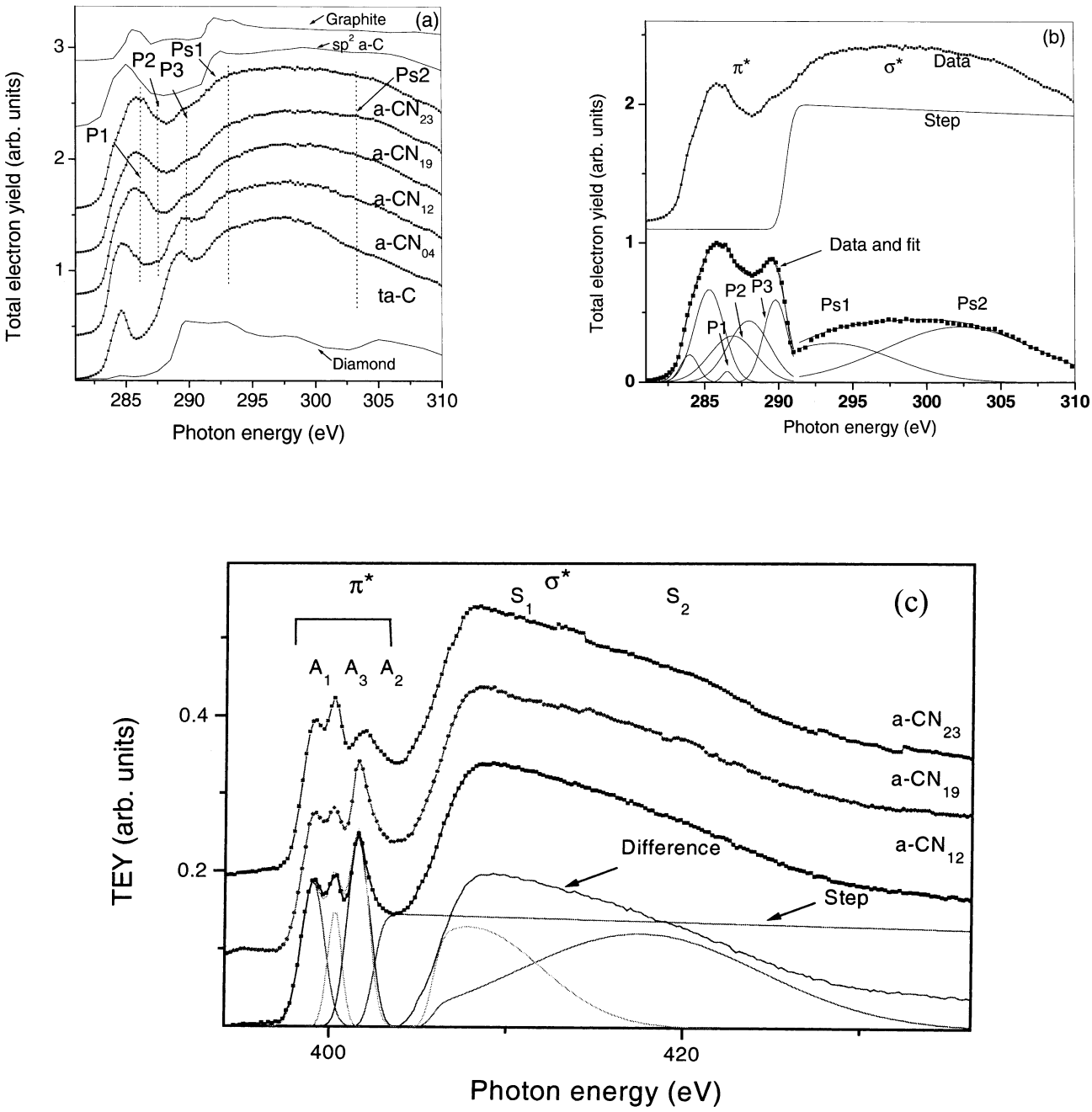

Fig. 1. (a) NEXAFS spectra of C K-edge of ta-C and a-CN_{4-23}, as well as diamond, graphite, and sp^2-bonded a-C [reproduced from Comelli et al., Phys. Rev. B 38 (1988) 7511]. (b) Decomposition of C K-edge of a-CN_{23}. (c) N K-edges of carbon films having different nitrogen concentration and decomposed N K-edge spectra of a-CN_{12}.

Obviously, these features are entirely different from graphite and sp^2 a-C, which show strong peaks at $\sim$285.5 ($1s \rightarrow \pi^*$) and 292 eV ($1s \rightarrow \sigma^*$).

Unlike the nitrogenated samples, a peak at 289.5 eV arises in ta-C due to core excitation at the onset of the $1s \rightarrow \sigma^*$ transition. For the same reason, this peak is also evident in the spectrum of a-CN_{04}, since the structure is close to ta-C. This peak also corresponds to the absorption edge of diamond (Fig. 1a) and lies in the gap between the π^* and σ^* peaks of other non-diamond-like nitrogenated samples. In this way, a clear distinction between the structure of ta-C and a-CN_x samples can be made. A peak at 287.9 eV is evident (Fig. 1a, in between P2 and P3 peaks) as a result of $1s \rightarrow \pi^*$ transitions for either C–H or C= [1–3], which is unlikely in the annealed films. We found similarity in terms of the position of peaks P1–P3 at the C K-edge with the decomposed peaks in the report by Jimenez et

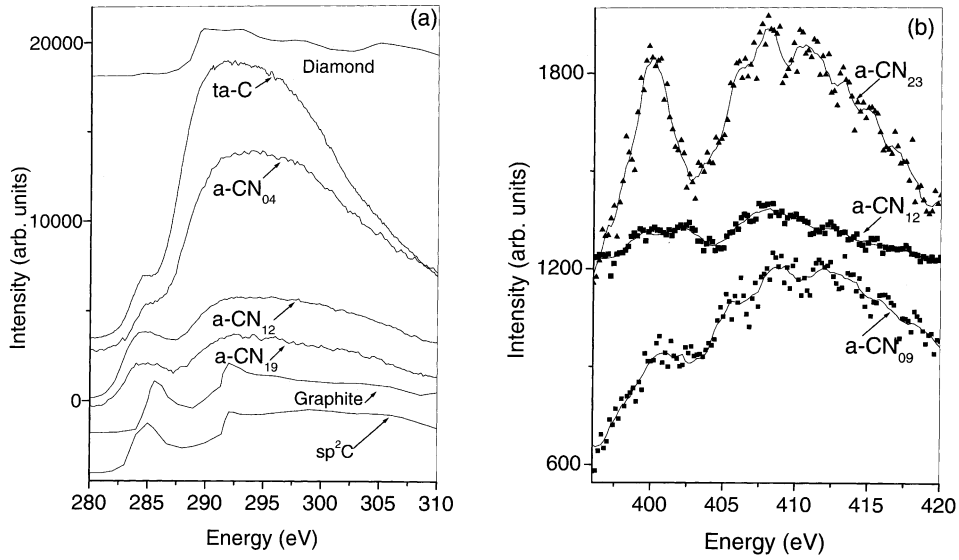

Fig. 2. EELS spectra of (a) C and (b) N K-edges of carbon films having different nitrogen concentrations.

al. [15]. From this report [15], the peak at 288 eV can be ascribed to weak C–N bonds in a metastable carbon nitride or carbon oxynitrile phase based on a carbon sp^2 hybrid. A peak at approximately 297 eV (see Fig. 1a) appearing from a $1s \rightarrow \sigma^*$ transition is very similar to crystalline diamond [1–3]. In diamond, the σ^* states are found to be localized in two energy regions, above and below the second bandgap lying at approximately 302.5 eV [1–3]. This feature, especially a dip (except a shallow minimum) at 302.5 eV, is not very clear in this or in a previous report [26]. Due to the high degree of disorder, band tailing and high defect density of states, the minimum at that energy is possibly almost filled up.

NEXAFS of a-CN_x films are compared with graphite and sp^2 a-C films. It is difficult to find exact similarity with these highly sp^2 a-C films, since the present a-CN_x films contain a large amount of nitrogen, unlike sp^2 a-C. A better comparison can be made with pyridine, which is presented in the following discussion. A major difference between the shape of the π^* peak in the C K-edge of the nitrogenated samples and the ta-C films has been found. The position of the π^* peak corresponding to the graphitic structure is found to be shifted in a-CN_{23} relative to ta-C. The intensity of the peaks at 283.9 and 284.6 eV increases with increasing nitrogen concentration and their positions slightly change as well (Fig. 1a). In a-CN_{04}, the peak maximum appears at approximately 285.5 eV and becomes very prominent for a-CN_{12}–a-CN_{23}, corresponding to the lowest-lying state of the π symmetry, near the center of the Brillouin zone of graphite (285.5 eV) [27,28]. The π^* antibonding state, or white band, for graphite is located at 285.5 eV and originates from the out-of-plane bonds in the sp^2 bonding configuration (Fig. 1a) [27–31].

In addition to graphite, simple structures of aromatic and nitrogen-containing organic molecules, e.g. benzene, pyridine and pyrrole, as well as nitrogen molecules, are considered for a comparative study between the NEXAFS spectra of these molecules and those of the present films. The width of the π^* peak increases with nitrogen concentration as additional peaks from the nitrogen-related structures, e.g. pyridine, evolve. Although in a-CN_{04} a small peak at approximately 285.9 eV appears, similar to the pyrrole molecule, the absence of a peak at 283.5 eV does not support the existence of a pyrrole-like structure in this sample.

On close inspection, humps can be identified at the C K π^* edge situated at approximately 283.9, 285.3, 286.5 (denoted as P1), 286.9 (P2), 287.9 and 289.8 eV (P3) (Fig. 1a,b). The position of these peaks has been primarily chosen from the humps or maxima appearing in the C K-edge spectra, as well as from the decomposition of the peak presented in our previous publication [32]. The position of the peaks is consistent with the features of graphite and pyridine and has been described earlier [15–20,32]. Briefly, for a-CN_{12}, a small peak at approximately 283.9 eV (pre-peak) appears very close to the π^* peak of ta-C. Apart from the first two peaks at 283.9 and 285.3 eV representing graphitic structure in the nitrogenated samples, in general, two peaks at approximately 286.5 (P1) and 286.9 eV (P2) (Fig. 1b) appear with the π^* character. Comparing P1 with benzene and pyridine, we find the π^* resonance for benzene appears at 285.9 eV and P2 corresponds to the $1s \rightarrow \pi^*(e_{2u})$ transition, similar to pyridine [27,28]. A peak with low intensity at approximately 289.8 eV (P3) indicates the $1s \rightarrow \pi^*(b_{2g})$ transition, almost similar to that of pyridine. This peak is not observed in graphite.

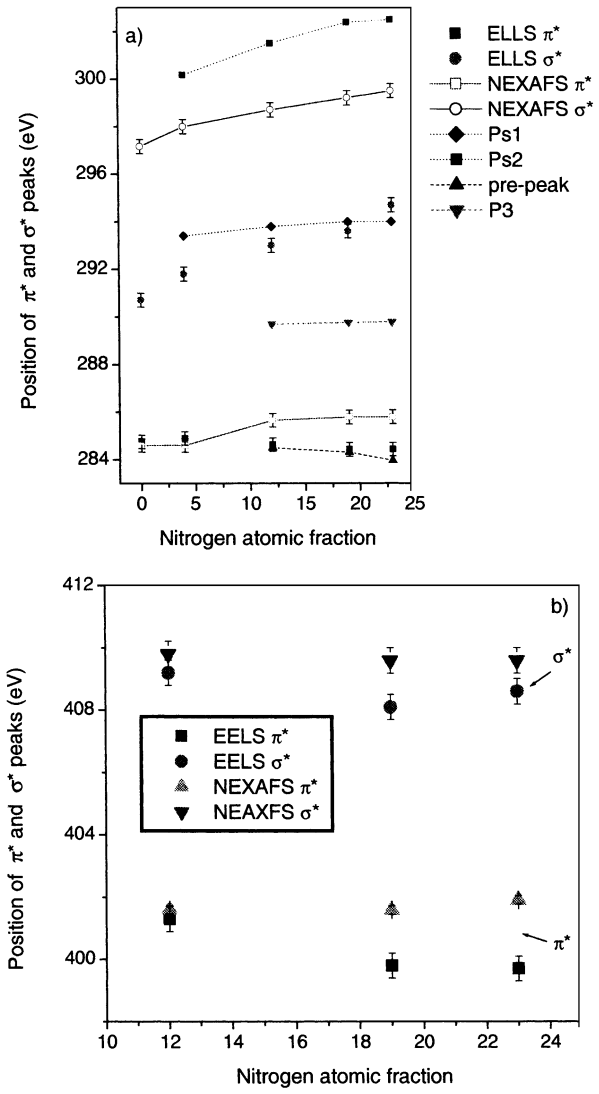

Fig. 3. Comparative study of the variation of the position of NEXAFS and EELS: (a) π* and σ* peaks at the C K-edge; and (b) π* and σ* peaks at the N K-edge as a function of the nitrogen concentration.

The σ* peaks of CN_x films are broad and the peak maxima are found to move towards high-energy regions as the nitrogen atomic fraction in the films increases (Fig. 3a). As the gross structure of nitrogenated carbon film is graphite-like, the chemical structure may be assumed to be analogous to pyridine, where one carbon atom in a hexagonal ring structure is substituted by a nitrogen atom, or to benzene. The σ* peaks were decomposed into two peaks, Ps1 and Ps2, in our previous report [32]. From the humps on the σ* peak in Fig. 1a, the position of Ps1 and Ps2 are determined (Fig. 1a). The position of Ps1 varies between 293.4 and 294 eV, which is very close to pyridine (293.8 eV). Broad features in the energy range between 300 and 302.5 eV (Ps2) also correspond to the σ* peak of benzene or pyridine, which should appear at 302.5 eV [23]. In particular, at the shallow minimum of ta-C at 302.5 eV, as discussed earlier, a peak (Ps2) appears from the pyridine structure of CN_x films. This similarity with pyridine becomes much more prominent in the N K-edge of the CN_x films. Therefore, first we describe the features already known from N K-edge of the pyridine molecule.

Pyridine has two unfilled π* orbitals (as in benzene) with e_{2u} (antibonding state where wave functions are antisymmetric) and b_{2g} (bonding state where wave functions are symmetric) symmetry giving rise to the peaks in N K-edge at 400 and 403.7 eV, respectively [4,27,28]. For a clear understanding of the CN bonding, the N K-edge of a-CN_{12} is decomposed (Fig. 1c). The position of the peaks has been determined from the position of maxima present in the N K-edge. All CN_x films show these decomposed π* peaks at approximately 399 (A1) and 401.6 eV (A2), although the energy difference of these peaks is not the same as that of pyridine. In pyridine, e_{2u} orbitals are split by 0.6 eV, and for the same reason, an intermediate peak at approximately 400.3 eV (A3) is noted in the present study. Along with the π* peaks, two σ* peaks at approximately 408 eV (S1) and a broad feature at approximately 417.6 eV (S2) are also observed and their position is very close to that of pyridine (see Fig. 1c and Table 2). The shape and position of the π* and σ* peaks in the N K-edge spectra change slightly at high nitrogen concentration (Fig. 3b).

On the other hand, we do not find similarity between CN_x films and pyrrole molecules. The intense peaks for pyrrole should appear at 286.4 and at 283.5 eV [1–3]. Also, there are dissimilarities between the N K-edge of CN_x films and pyrrole molecules, in particular the absence of the π* and σ* peaks at 398.5 or 401.2, 403 (π*), 408 (σ* band from C–N) and 413 eV (σ* band from C–C) in the CN_x films that are commonly observed for pyrrole. From these features, it can be concluded that the concentration of pyrrole-based molecules on the surface of CN_x films is very low and not detectable by this technique [29]. Summarizing the features of the C and N K-edge spectra of the CN_x films, we find that they are very similar to that of deposits of benzene and pyridine, although the sharp features are smoothed out at the edges (Table 2) [23].

In order to understand the bonding arrangement of the CN molecules, the intensity ratio of the σ* and π* peak in the C and N K-edges has been calculated (see Fig. 4a,b and Fig. 1a). It is found that at the C K-edge, this ratio declines from ta-C film to a-CN_{04} and then saturates. On the other hand, in the N K-edge at high nitrogen concentration, a sharp decrease in this ratio is observed. This means that the percentage of the C=N bond, and therefore the concentration of pyridine molecules on the film surface, increases with nitrogen concentration.

The intensity of an NEXAFS peak is a product of the density of final states $[Q_f(E)]$ and the transition probability of an electron from a core ($|i>$) to an excited state ($|f>$). Considering dipole approximation, the X-ray absorption cross-section is described by:

$$\sigma_x = (h^2/m^2) \times (2\pi e^2/hc)\left(2\pi/h\omega\right)|<f|e\cdot p|i>|\_Q_f(E) \quad (1)$$

where e and p represent a unit vector of photon flux and sum of the linear momentum operators of electrons, respectively [21,22]. In practice, it is very difficult to calculate the density of unoccupied states from a material different from metal, even for graphite. This is due to the core-hole created by the absorption process being much less screened in non-metals than metals, and a strong interaction of the unoccupied states with the core-hole takes place [30]. X-Ray absorption at a particular photon energy is proportional to the square of the overlap integral of the excited-state wavefunction with the core-level wavefunction, which should be highly specific to the way nitrogen atoms are bonded into the network [21,22]. In a particular edge (C or N K) the atoms (C or N) forming a π or σ bond with neighbors will show a strong π^* or σ^* peak, respectively. In both of the edges, the intensity ratio of σ^*/π is greater than 1, indicating that there is a greater amount of σ than π bonds. Since nitrogen cannot form a hexagonal ring structure alone, but substitutes for one carbon atom in the hexagonal ring, then the percentage of N=C (or N=N) bonds relative to C–N (or N–N) bonds must increase as the nitrogen concentration in the films increases. In addition, the sharp A3 peak at the N K-edge of a-CN_{23} is a good indication of a high concentration of C=N bonds, as well as of pyridine molecules in this film. The intensity of the N K-edge relative to the C K-edge may change due to the charge transfer, as indicated by Wan and Egerton [31].

If the nitrogen atoms are in substitutional sites, then the C and N K-edges should have a similar appearance, neglecting the effect of charge transfer from C to N atoms. For the non-substitutional sites, a difference between the near edge spectra should occur. If nitrogen atoms form a doping configuration in the carbon matrix, then the excited-state wavefunction will also have a large amplitude. The dissimilarity of the σ^*/π^* ratio

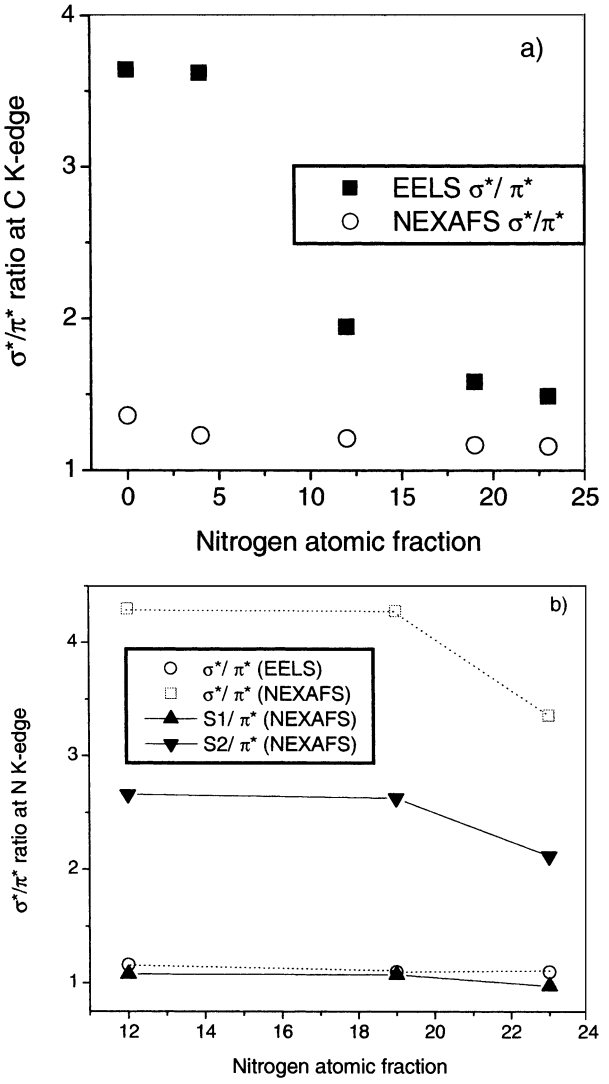

Fig. 4. Comparative study of the variation of the intensity ratio of σ^*/π^* at (a) the C K-edge and (b) the N K-edge as a function of the nitrogen concentration.

Table 2
Comparison of the position of peaks observed from the C and N K-edges of different organic molecules, nitrogen and CN_x films

	C K-edge (eV)				N K-edge (eV)			
	$1s\rightarrow\pi^*(e_{2u})\pi^*(b_{2g})$		$1s\rightarrow\sigma^*(e_{2u})\sigma^*(b_{2g})$		$1s\rightarrow\pi^*(e_{2u})\pi^*(b_{2g})$		$1s\rightarrow\sigma^*(e_{2u})\sigma^*(b_{2g})$	
	(P1)	(P2)	(Ps1)	(Ps2)	(A1)	(A2)	(S1)	(S2)
Benzene	285.9	289.6	295	302	–	–	–	–
Pyridine	284.5	289.5	293.8	302.5	400	403.8	410	416
CN_x	285.5	286.5	293.8	301–304	399–402		408	417
N_2, N_2^+	–	–	–	–	400–400.9		402–415	

between the C and N K-edges suggests that the environment of the nitrogen atoms is different from that of the carbon atoms. Thus, not all nitrogen atoms can be expected to substitute carbon atoms in the network and nitrogen is not subtitutionally doped in the carbon films. Consequently, the atomic fraction of nitrogen in a locally ordered CN_x structure would be different from disordered structure.

3.2. K-edges from EELS

A very significant change in the C and N K-edges of the samples is observed as a function of nitrogen content (see Fig. 2a–c andFig. 3a,b). The area and shape of the π^* and σ^* peaks vary with nitrogen concentration. The C K-edge of the samples is compared to diamond, graphite and sp^2-bonded a-C films. Features of ta-C films are similar to diamond to some extent, establishing a high concentration of sp^3-bonded carbon. The position of the σ^* peak in ta-C is similar to diamond, although no sharp feature has been observed. In ta-C, the π^* peak is also observed due to the presence of sp^2-bonded carbon. This peak becomes intense with increasing nitrogen concentration compared to the respective σ^* peak observed in sp^2-bonded carbon. Although at high nitrogen concentration the N K-edge is very intense and the intensity of σ^* and π^* can be easily quantified, this is difficult at low nitrogen concentration due to the low intensity of these peaks. A significant difference in the line shape of the π^* and σ^* peaks implies that the concentrations of C–N and C=N bonds are different.

The change in position of the C and N K-edges of the samples as a function of nitrogen content is presented in Fig. 3a,b. The π^* peak at the C K-edge starting from approximately 284.5 eV for ta-C moves slightly towards the high-energy side in the low nitrogen-concentration region (i.e. up to approx. 10%), followed by a shift towards the low-energy region with increasing nitrogen concentration. In contrast, the σ^* peak is found to be displaced to the high-energy side uniformly with nitrogen concentration (Fig. 3a). The variations of the π^* and σ^* peaks in the N K-edge are generally smaller than for the C K-edge (Fig. 3b).

The σ^*/π^* peak intensity ratio was calculated from the C and N K-edges (Fig. 4a,b). At the C K-edge, the decrease in this ratio is monotonous (Fig. 4a), indicating that the percentage of C sp^2 bonds increases compared to carbon sp^3 bonds with increasing nitrogen concentration. Due to poor resolution of the EELS C K-edge, decomposition of the C K-edge was not possible. The N K-edge shows an overall improvement in intensity of π^* compared to σ^* with nitrogen concentration, suggesting an increase in the amount of C=N relative to C–N bonds (Fig. 4b).

We have discussed in the previous sub-section that the similarity of π^* peaks between the N and C K-edges might indicate that nitrogen is substitutional in all networks, ranging from a tetrahedral to a trigonal structure. In the present study, the intensity ratios at the N and C K-edges are not constant, having different nitrogen concentration (Fig. 4b). The intensity of the π^* peak is comparable to the σ^* peak in the N K-edge, but the π^* peak is much less intense relative to the σ^* peak in the C K-edge. It is understood that with increasing nitrogen atomic fraction, the substitutional fraction of carbon atoms in the sp^2-bonded network becomes higher.

3.3. Comparative study of NEXAFS and EELS

In the EELS experiment, the samples are approximately 50 nm thick for efficient electron transmission, whereas in NEXAFS, the escape depth of the electrons is approximately 3.5 nm in the total electron yield mode, which provides information on the samples near to the surface. For this reason, a difference in the sample properties measured from these two experiments may be noted. A very interesting change in the intensity of A1, A2 and A3 peaks at the NEXAFS N K-edge with respect to the σ^* peak has been observed as the nitrogen concentration in the films increases. In all the films studied, the intensity of the π^* peak for the NEXAFS N K-edge is lower than the respective σ^* peak. It may be noted that this relative change takes place mostly due to the contribution of A3 and not of the other two peaks. A very similar type of trend was reflected from the EELS N K-edge.

The variation of the position of the π^* peak of the EELS and NEXAFS C K-edge with nitrogen fraction is found to be almost similar (Fig. 3a). An identical trend of the variation of the position of σ^* peak, with a difference in their absolute values, has been observed. The variation of the pre-peak, P3, Ps1 and also Ps2 peaks (from Fig. 1a) is demonstrated in Fig. 3a. A slight shift of the pre-peak towards the low-energy side has been observed as the nitrogen concentration increases. Similarly, Ps1 and Ps2 peaks move towards the high-energy region with increasing nitrogen concentration. In general, movement of the Ps1 peak is very consistent with that of the σ^* peak, as observed from the EELS spectra (Fig. 3a). The relative intensity of the σ^* peak decreases with increasing nitrogen concentration in the films (Fig. 4a), indicating an increase in graphitization of the samples. The position of the π^* and σ^* peaks at the N K-edge of the samples has been compared and no great displacement has been observed (Fig. 3b). In particular, the position of the π^* peak in the EELS spectra decreases slightly as a function of nitrogen concentration. The position, as well as the relative intensity, of the decomposed components of the π^* and σ^* peaks is, to some extent, similar to that of the NEXAFS N K-edge. At the N K-edge, the σ^*/π^* ratio

is found to be different to that of the C K-edge, which decreases with nitrogen concentration (Fig. 4b). Hence, a difference in both the local structure and the environment of the C and N atoms can be established.

4. Conclusions

NEXAFS spectroscopy is found to be a powerful technique to interpret fine structure from the N K-edge of CN_x films. The contribution from CN bonds and nitrogen in the CN_x films has been separated from the graphitic structure. The short-range order of the nitrogenated carbon films prepared using a vacuum arc is found to be similar to that of pyridine molecules. From curve-fitting of the N K edges, contributions from different bonding and anti-bonding state transitions have been shown. Combined with EELS, as both yield a similar physical interpretation, a concrete analysis of the film structure has been carried out. A remarkable similarity between NEXAFS and EELS data has been found. The amount of C=N compared to C–N bonds increases with increasing nitrogen concentration in the films. From the variation of the position and intensity of different decomposed peaks at the N K-edge, changes in carbon- and nitrogen-related structures have been interpreted.

Acknowledgements

The first author would like to thank the Alexander von Humboldt Foundation for financial assistance.

References

[1] J. Stöhr, NEXAFS Spectroscopy, Springer, New York, 1992.
[2] G. Comelli, J. Stöhr, C.J. Robinson, W. Jark, Phys. Rev. B 38 (1988) 7511.
[3] C. Lenardi, P. Piseri, V. Briois, C.E. Bottani, A.L. Bassi, P. Milani, J. Appl. Phys. 85 (1999) 7159.
[4] M. Bader, J. Hasse, K.-H. Frank, A. Puschmann, A. Otto, Phys. Rev. Lett. 56 (1921) 1986.
[5] E. Demuth, K. Christmann, P.N. Sanda, Chem. Phys. Lett. 76 (1980) 201.
[6] A. Otto, K.–H. Frank, B. Reihl, Surf. Sci. 163 (1985) 140.
[7] G. Contini, A. Ciccioli, C. Laffon, P. Parent, G. Polzonetti, Surf. Sci. 412/413 (1998) 158.
[8] N.A. Booth, R. Davis, D.P. Woodruff, et al., Surf. Sci. 416 (1998) 448.
[9] H.C. Holloway, D.K. Suuh, M.A. Kelly, et al., Thin Solid Films 290/291 (1996) 94.
[10] F.L. Coffman, R. Cao, P.A. Pianetta, S. Kapoor, M. Kelly, L.J. Terminello, Appl. Phys. Lett. 69 (1996) 568.
[11] J. Robertson, C.A. Davis, Diamond Relat. Mater. 4 (1995) 441.
[12] S. Bhattacharyya, O. Madel, S. Schultze, M. Heitschold, P. Haüssler, F. Richter, Phys. Rev. B 61 (2000) 3927.
[13] S. Bhattacharyya, M. Heitschold, F. Richter, Diamond Relat. Mater. 9 (2000) 544.
[14] S. Bhattacharyya, U. Starke, F. Richter, Appl. Phys. Lett., submitted.
[15] I. Jimenez, W.M. Tong, D.K. Shuh, et al., Appl. Phys. Lett. 74 (1999) 2620.
[16] N.M.J. Conway, A. Ilie, J. Robertson, W.I. Milne, A. Tagliaferro, Appl. Phys. Lett. 73 (1998) 2456.
[17] T.A. Friedmann, K.F. McCarty, J.C. Barbour, M.P. Siegal, D.C. Dibble, Appl. Phys. Lett. 68 (1996) 1643.
[18] A.C. Ferrari, B. Kleinsorge, N.A. Morrison, A. Hart, V. Stolojan, J. Robertson, J. Appl. Phys. 85 (1999) 7191.
[19] J.V. Anguita, S.R.P. Silva, A.P. Burden, et al., J. Appl. Phys. 86 (1999) 6276.
[20] M. Zhang, Y. Nakayama, S. Harada, J. Appl. Phys. 86 (1999) 4971.
[21] C.A. Davis, D.R. Mckenzie, L.E. Hall, et al., J. Non-Cryst. Solids 170 (1994) 46.
[22] C.A. Davis, D.R. McKenzie, L.E. Hall, et al., Philos. Mag. B 69 (1994) 1133.
[23] T. Tyliszczak, F. Esposto, A.P. Hitchcock, Phys. Rev. Lett. 62 (1989) 2551.
[24] J. Kikuma, K. Yoneyama, M. Nomura, et al., Electron Spectrosc. Relat. Phenom. 88–91 (1998) 919.
[25] I. Gouzman, A. Hoffman, G. Comtet, L. Hellner, G. Dujardinand, M. Petravic, Appl. Phys. Lett. 72 (1998) 2517.
[26] S. Anders, J. Diaz, J.W. Agerill, Appl. Phys. Lett. 71 (1997) 3367.
[27] R.A. Rosenberg, P.J. Love, V. Rehn, Phys. Rev. B 31 (1984) 2634.
[28] D. Denley, P. Perfetti, R.S. Williams, D.A.. Shirley, J. Stöhr, Phys. Rev. B 21 (1980) 2267.
[29] G. Tourillon, S. Raaen, T.A. Skotheim, M. Sagurton, R. Garrett, G.P. Williams, Surf. Sci. 184 (1987) L345.
[30] J. Fink, T. Müller-Heinzerling, J. Pflüger, et al., Phys. Rev. B 34 (1996) 1101.
[31] L. Wan, R.F. Egerton, Thin Solid Films 279 (1994) 34.
[32] S. Bhattacharyya, M. Lubbe, F. Richter, J. Appl. Phys. 88 (2000) 5043.